

SYNTHESIS AND CHARACTERIZATION OF IRON OXIDE NANOPARTICLE FROM $FeCl_3$ BY USING POLYVINYL ALCOHOL

Sanjay Srivastava*

Abstract:

This work has been focused on the synthesis of the iron oxide nano particle from the spanich (In Hindi: palak) by using polyvinyl alcohol in static and dynamic state. The sizes of the nano particle were determined by XRD technique. The presences of the functional group in iron oxide nano particle were characterized through FTIR. LVSEM and EDAX were carried to examination the surface feature and determine the chemical composition of the nano particle. The decomposition of the feric oxide was studied by TG analysis. The result shows that the magnetite nano powders were successfully prepared by chemical route in polymer matrix. The dynamic state modifies the size particle by repeating of impact. This method has the advantage that it can produce ultra-fine iron oxide powder quickly. The prolonged thermal treatment of the Fe_3O_4 produced Fe_2O_3 hematite nano particle. The sizes of the nano particle are found approximately 44.6 in static state and 20nm in dynamic state analyzed through XRD. EDAX and FTIR analysis show the presence of the respective element and their functional group.

Key words: Hematite, magnetite nano particle, PVA, FTIR, LVSEM, EDAX, SEM

* Materials Science & Metallurgical Engineering, Maulana Azad National Institute of Technology, Bhopal-462051.

1. Introduction:

Many different types of lohas (metals) are quoted in ancient literature for their medicinal values through many metals. Out of these reduced iron/oxide show important aspect in auyurvedic medicine. Iron (III) oxide (Fe_2O_3) or ferric oxide is also chemically known as hematite (alpha form) or magnetite (gamma form) in its mineral form. But in ancient medicine it is known as loha bhasm. As an industrial chemical it is commonly called rouge. Now a days in purified, it is used as a coating in magnetic audio and computer media. In a dry or alkaline environment, it can cause passivation and inhibit rust, yet it is also a major component of rust and dried blood. Iron (III) oxide is also used as a pigment, under names Pigment Brown 6, Pigment Brown 7, and Pigment Red 101. Some of them, e.g. Pigment Red 101 and Pigment Brown 6, are Food and Drug Administration (FDA)-approved for use in cosmetics [1]. The latest developments in functionalized magnetic nano-particles show considerable promise for both enhanced and novel application such as (1) catalyst, (2) pigment, (3) sintering, (4) photonic, (5) drug, and (6) biomedical products. Juliano Toniolo [2] described the solution combustion synthesis technique as applicable to iron oxide powder production using urea as fuel and ferric nitrate as an oxidizer. Song Lixian [3] introduced citrate ions as a complex compound in the co-precipitation method for ultrafine magnetite nanoparticle preparation. Well dispersed Fe_3O_4 nano-particle were directly prepared. H. Namduri [4] studied a systematic approach based on the application of Fourier transform infrared spectrometry (FTIR) was taken in order to quantitatively analyze the corrosion products formed in the secondary cycle of pressurized water reactors (PWR). Ming Ma [5] studied magnetite nanoparticles which were prepared by co-precipitation of Fe^{2+} and Fe^{3+} with NH_4OH , and then, amino silane was coated onto the surface of the magnetite nanoparticles. Mizutani [6] studied magnetite nanoparticles prepared by hydrothermal synthesis under various initial ferrous/ ferric molar ratios without adding any oxidizing and reducing agents in order to clarify effects of the molar on the reaction mechanism for the formation of magnetite nano particles. Zhao Yuanbi [7] prepared Fe_3O_4 magnetic nanoparticles by the aqueous co-precipitation of $\text{FeCl}_3 \cdot 6\text{H}_2\text{O}$ and $\text{FeCl}_2 \cdot 4\text{H}_2\text{O}$ with addition of ammonium hydroxide. The conditions for the preparation of Fe_3O_4 magnetic nanoparticles were optimized, and Fe_3O_4 magnetic nanoparticles obtained were characterized systematically by means of transmission electron microscope (TEM), dynamic laser scattering analyzer (DLS) and X-ray diffraction (XRD). The results revealed that the magnetic nanoparticles were cubic shaped and dispersive, with narrow size distribution and average diameter of 11.4 nm.

R. Y. Hong [8] introduced, methods to synthesize magnetic Fe_3O_4 nanoparticles and to modify the surface of particles are presented in the present investigation. Fe_3O_4 magnetic nanoparticles were prepared by the co-precipitation of Fe^{3+} and Fe^{2+} , $\text{NH}_3 \cdot \text{H}_2\text{O}$ was used as the precipitating agent to adjust the pH

value, and the aging of Fe_3O_4 magnetic nanoparticles was accelerated by microwave (MW) irradiation. The average size of Fe_3O_4 crystallites was found to be around 8–9 nm.

Y. F. Shena [9] studied Fe_3O_4 magnetic nanoparticles with different average sizes were synthesized and structural characterizations showed that the three kinds of nanoparticles had different sizes, *i.e.*, an average particle size of 8 nm, 12 nm and 35 nm was observed for the nanoparticles prepared with the co-precipitation method, the co-precipitation combining a surface decoration process, and the polyol process, respectively. The synthesized Fe_3O_4 nanoparticles with different mean particle sizes were used for treating the wastewater contaminated with the metal ions, such as Ni (II), Cu (II), Cd (II) and Cr(VI). It is found that the adsorption capacity of Fe_3O_4 particles increased with decreasing the particle size or increasing the surface area. Various factors influencing the adsorption of metal ions, *e.g.*, pH, temperature, amount of adsorbent, and contacting time were investigated to optimize the operation condition for the use of Fe_3O_4 nanoparticles with an average size of 8 nm. The obtained results indicated that the mechanism was strongly influenced by the pH and temperature of wastewater. The maximum adsorption occurred at pH 4.0 under room temperature (20°C) and the adsorption capacity of Fe_3O_4 nanoparticles was as high as 35.46 mg/g, which is almost 7 times higher than that of the coarse particles.

Jie Chen [10] studied Fe_3O_4 nanoparticles with different morphology such as sphere, nanowire, biscuit-like and quasi-cubes were successfully prepared using a simple hydrothermal method. The products were characterized by powder X-ray diffraction (XRD), scanning electron microscope (SEM) and transmission electron microscopy (TEM). The results showed that the morphology of product can be adjusted by changing the reaction conditions such as reaction time, different amount of surfactant added and the addition of organic solvent. In addition, the possible mechanism for the formation of different morphology under the corresponding reaction condition was suggested. In this present work the Iron oxide are being produced by chemical route from spinach by using poly vinyl alcohols matrix in static and dynamic state.

2. Experimental Methods:

2.1. Material used

0.2702 g iron(III) chloride (Across Organics, Berlin AR grade), 0.1988 g iron (II) chloride tetrahydrate (Fluka, AR grade), 8 ml aqueous ammonia (Rankem, AR grade) solution, 150 ml distilled

water as solvent and aqueous solution of polyvinyl alcohol with different content were chosen for the preparation.

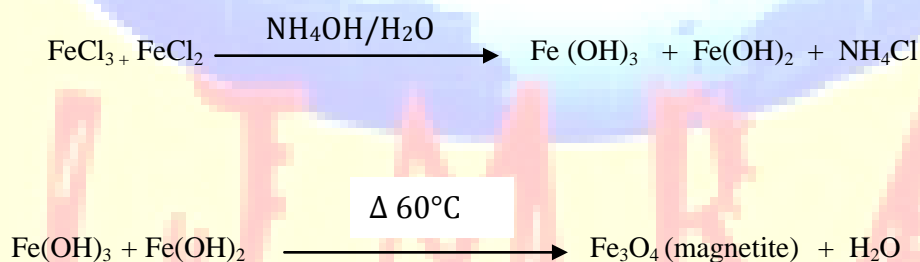
2.2 Synthesis

The iron oxide was extracted from spinach. Spanish content appropriate amount of calcium and iron. 150 ml distilled water was taken in a 250 ml three necked round bottom flask. It was degassed with Ar gas for 10 min.

The 10 gram of FeCl_3 was dissolved in 150 ml of distilled water. The extractions were occurred by the addition of aqueous solution of hydrochloric acid in spinach solution. 20 ml ammonia solution was added drop by drop into it. The variable concentrations of poly vinyl alcohol were added in spinach solution. The concentration of polyvinyl varies from 2 to 10 %.

The mixture was stirred from mixer and grinder at 345rpm for 1 hour under heating in a water bath at 60°C . The mixture was allowed to settle & cooled. The black colored product obtained was washed several times with 20 ml of distilled water each. Then it was washed similarly with 10 ml methanol for 3 times. The obtained product was air dried and weighed. Yield: 0.1999 g.

2.3. Reaction



Magnetite nano particles when heated at 300°C for 4 hour then reddish-brown solid particles was found which was found to be hematite nano particles [Fig. 4].



2.4. Instrumentation

The sizes of the nano particle were determined through XRD. The radiation source used was $\text{CuK}\alpha$ and the nickel filter was used to block $\text{K}\beta$ radiation. XRD analysis was also carried for the phase analysis. The decomposition of magnetite was studied by TGA. Electronic pan balance was used to

measure the change in weight. Iron oxide nanoparticles so obtained were characterized by scanning electron microscope (SEM), energy dispersive analysis of X-ray (EDAX), FT-IR (Fourier transform infrared spectrophotometry).

Fourier transform infrared (FT-IR) spectra were taken on the powder samples in a Perkin Elmer RX I Spectrometer as a solid KBr disc in the range 4000-400 cm^{-1} . Scanning Electron Microscopy (SEM) images were obtained on thin film of the sample spin-coated (@1400 RPM) on a cleaned silicon wafer in a CARL-ZEISS EVO 50 XVP Low Vacuum Scanning Electron Microscope (LVSEM) equipped with Everhart-Thornley SE detector. The samples were coated with gold to make conductive. Energy Dispersive Analysis of X-ray (EDAX) analyses was done with a Genesis 2000 ED System having a resolution of 135 eV.

3. Result and discussion:

3.1 XRD measurement

1. (A) Size measurements of Magnetite

The formula for magnetite may also be written as $\text{FeO}\cdot\text{Fe}_2\text{O}_3$, which is one part wustite (FeO) and one part hematite (Fe_2O_3). This refers to the different oxidation states of the iron in one structure, not a solid solution. The grain size of the crystallite (diameter D) was determined from the full width at half maximum ($\Delta\omega_\theta$) of the peaks by using the Scherrer formula.

$$D = K \lambda / (\Delta\omega_\theta) \text{Cos } \theta_B$$

Where θ_B is the Bragg angle and λ is the X-Ray wavelength. Here $K = 0.89$ is for spherical shape. For calculation ($\Delta\omega_\theta$) is observed by zooming the peak position using origin graphics software. The XRD scanning from 10° - 70° shows the lines (220), (311), (400), (422), (511), and (440) at $2\theta = 31.275^\circ, 36.755^\circ, 44.915^\circ, 54.789^\circ, 57.695^\circ,$ and 63.265° , respectively for Fe_3O_4 . The calculated size of the iron oxide nano particle is tabulated in Table 1 as follows:-

Table 1 : Particle size calculation by using Scherrer formula in different concentration

S.No.	Name of Sample	ppm of the solution (mg/L)	Size in static condition	Size in dynamic condition (300 rpm)

1	Fe ₃ O ₄ (MG1)	200	72.6	71.3
2	Fe ₃ O ₄ (MG2)	500	77.8	79.33
3	Fe ₃ O ₄ (MG3)	1000	81.8	82.2
4	Fe ₃ O ₄ (MG4)	2000	86.7	85.4
5	Fe ₃ O ₄ (MG5)	4000	99.2	89.9

Table 2: Particle size calculation by using Scherrer formula in different PVA concentration.

S.No.	Name of Sample	PVA (%)	Size in static condition	Size in dynamic condition (300 rpm)
1	Fe ₃ O ₄ (MG1)	2	82.6	77.3
2	Fe ₃ O ₄ (MG2)	4	81.8	77.33
3	Fe ₃ O ₄ (MG3)	6	80.8	75.2
4	Fe ₃ O ₄ (MG4)	8	80.7	72.4
5	Fe ₃ O ₄ (MG5)	10	77.2	69.9

1. (B) Size measurement of Hematite

The calculated size of the iron oxide nano particle (Hematite) after prolonged heating (6 hrs) in electric arc furnace by using debye scherrer formula is tabulated in Table 2 as follows. It can be found that the mean size of the particle before heating with variable percentage of PVA is varied from 82.6 to 77.2 nm in static condition and 77.3 to 66.9 nm in dynamic condition which was almost unchanged after prolonged heating (6hrs). The XRD scanning from 10°-70° shows the lines (150) and (315), at $2\theta = 44.930^\circ$ and 61.010° , respectively for Fe₂O₃ (monoclinic) and lines (204), (206), (109), (313), (0012), (1012), (2212), (0015), and (2114) at $2\theta = 25.275^\circ$, 30.355° , 33.415° , 35.695° , 43.265° , 44.930° , 53.590° , 54.365° and 57.210° , respectively for Fe₂O₃ (tetragonal). The observation of a diffraction peak for the iron oxide nanoparticles indicates that these are tetragonal and monoclinic. However, the predominance of the (150) and (315) line in XRD indicates reorientation of the Fe₂O₃ (monoclinic) nanoparticle preferentially in two directions as against the random orientation of grains in the bulk material. For Fe₂O₃ (tetragonal) nanoparticles have the predominance of the (204), (206), (109), (313), (0012), (1012), (2212), (0015), and (2114) line in XRD indicates reorientation of the nanoparticle preferentially in nine directions. From the

full width at half maximum, the average crystalline size can be estimated with the (315), and (0012) diffraction peaks in the XRD spectra according to the Scherrer formula $d = KA/(B\cos\theta)$, d is the crystallite size; $K = 0.89$, which is the Scherrer approximate constant related to the shape and index (hkl) of the crystals; A is the wavelength of the X-ray (Cu $K\alpha$, 0.154 nm); θ is the diffraction angle; and B is the corrected half-width of the diffraction peak (in radians) given by $B^2 = B_m^2 - B_s^2$; where B_m is the measured half-width and B_s is the half-width of a standard sample with a known crystal size greater than 100 nm. The calculated average crystallite sizes are around 69.5 nm for Fe_2O_3 (monoclinic) nanoparticle and 74.7 nm for Fe_2O_3 (tetragonal) [11].

Table 3 : Particle size calculation by using Scherrer formula in different concentration

S.No.	Name of Sample	ppm of the solution (mg/L)	Size in static condition	Size in dynamic condition (300 rpm)
1	FeO. Fe_2O_3 (HT1)	200	72.6	71.3
2	FeO. Fe_2O_3 (HT2)	500	74.8	79.33
3	FeO. Fe_2O_3 (HT3)	1000	81.8	82.2
4	FeO. Fe_2O_3 (HT4)	2000	83.7	75.4
5	FeO. Fe_2O_3 (HT5)	4000	92.2	83.9

Table 4. Particle size calculation by using Debye scherrer formula in different PVA concentration

S.No.	PVA (%)	Reaction sequence	Size in static condition	Size in dynamic condition (300 rpm)
1	2	$Fe_3O_4 \longrightarrow FeO. Fe_2O_3$ (HT1)	82.6	77.3
2	4	$Fe_3O_4 \longrightarrow FeO. Fe_2O_3$ (HT2)	81.8	77.33
3	6	$Fe_3O_4 \longrightarrow FeO. Fe_2O_3$ (HT3)	80.8	75.2
4	8	$Fe_3O_4 \longrightarrow FeO. Fe_2O_3$ (HT4)	80.7	72.4
5	10	$Fe_3O_4 \longrightarrow FeO. Fe_2O_3$ (HT5)	77.2	69.9

3.2. Fourier transformation spectra

Sample powders were added to dry KBr powder and compressed in to pellets using a hydraulic press. Magnitude of compression applied in KBr pellet preparation needs to be kept constant to

avoid variation in absorbance intensity from one sample to the next. Two equivalent runs of each of the two samples were made on the FT-IR spectrometer.

Fig. 5 and 6 represent the FT-IR spectra of magnetite and hematite respectively. It has been observed that the absorption band at a high wave number region is due to the OH stretching which suggests that the surfaces of the Fe_3O_4 nano-particles are covered with a number of hydroxyl (-OH) groups as is obvious and well-reported when they are prepared in the aqueous phase. $\nu(\text{OH})_{\text{str}}$ and $\delta(\text{OH})$ were obtained at 3423.43 and 1620.27 cm^{-1} respectively for magnetite whereas at 3394.31 and 1624.17 cm^{-1} respectively for hematite. As shown in the Fig. 5 and 6, the Fe-O stretching vibration of the tetrahedral and octahedral lattice site was found at 574.04 cm^{-1} for magnetite which is shifted to the lower wave number at 564.40 cm^{-1} in hematite. Presence of two other absorption bands at 628.57 cm^{-1} and 429.49 cm^{-1} indicates the defects in the lattice of the hematite. As reported in the literature, the FT-IR spectrum of magnetite should exhibit also two other absorption bands near 268 cm^{-1} and 178 cm^{-1} but these bands were beyond the detection limit of our instrument.

3.3 scanning electron Microscopy

Fig. 7 and 4 show representative SEM images of the magnetite nano-particles and their thermally treated product. Estimation of the particle size appeared very difficult for the samples reported herein specially because of their extremely small dimension and inherent nature of agglomeration which is obvious due to high dipole-dipole interactions among the uncapped nano-particles. It can be found in SEM images that the particles are more or less spherical in nature having an average size of $\sim 100\text{ nm}$.

It can be clearly observed from Fig. 4 that the larger Fe_3O_4 nano-particles are rough in appearance and composed of relatively small Fe_3O_4 nano-particles indicating that the Fe_3O_4 nano-particles are self-assembled into higher aggregates.

The SEM observation also indicated that the mean size of the particles before heating was $\sim 100\text{ nm}$ which is almost unchanged in the particles after prolonged heating for 4 hrs.

3.4. Energy dispersive analysis

EDAX studies on the magnetite sample were carried out in a CARL-ZEISS EVO 50 XVP Low Vacuum Scanning Electron Microscope (LVSEM)-EDAX instrument equipped with Genesis 200 Energy Dispersive system which reveals that the elemental composition of the samples is Fe and O. Fig. 5 represents the EDAX spectrum of the magnetite sample. Anal. Calcd (found) for Fe_3O_4 : Fe, 72.36 (72.27); O, 27.64 (27.73) %. The obtained result correlates well qualitatively as well as quantitatively with the desired compound.

3.5. X-ray photoelectron spectroscopic analysis

The iron oxidation states with X-ray photoelectron spectroscopy (XPS) can be obtained the Fe2p_{3/2} (710.4 eV) and Fe2p_{1/2} (724.2 eV) for Fe₂O₃ and the Fe2p_{3/2} (711.3 eV) and Fe2p_{1/2} (725.0 eV) for Fe₃O₄. The high binding energy of Fe2p_{3/2} for Fe₃O₄ as compared with Fe₂O₃ is originated from Fe²⁺ ion. [12].

3.6. UV-visible spectroscopy

(a) UV-visible spectroscopy of magnetite

The UV-Vis absorption spectra of different samples in n-hexane prepared in different condition with particle sizes are illustrated in Fig. 10. The data is plotted in static as well as in dynamic condition. And their result was tabulated in Table 5(a) and (b). 1st and 2nd absorption peaks are shifted towards higher wavelength side with increasing of sizes of hematite. In PVA matrix, the size of the nanoparticles of magnetite gets reduced. It is evident from the Fig.10 that the absorption peaks are slightly shifted towards higher energy sides. Preparation of nanoparticles of magnetite either in dynamic or static condition changes only the sizes of prepared materials. From static to dynamic condition of preparation of nanoparticles, only blue shift is observed.

Table 5(a): 1st and 2nd UV-vis peak position with particle size in static condition (in different conc. of FeCl₃)

S.No.	Name of Sample	ppm of the solution (mg/L)	Size in static condition	UV-Vis date of magnetite in 1 st absorbance	UV-Vis date of magnetite in 2 nd absorbance
1	Fe ₃ O ₄ (MG1)	200	72.6	245.9	652.5
2	Fe ₃ O ₄ (MG2)	500	77.8	251.2	661.5
3	Fe ₃ O ₄ (MG3)	1000	81.8	255.3	669.8
4	Fe ₃ O ₄ (MG4)	2000	86.7	258.4	673.3
5	Fe ₃ O ₄ (MG5)	4000	99.2	261.3	682.5

Table 5(b) : 1st and 2nd UV-vis peak position with particle size in dynamic condition

S.No.	Name of Sample	ppm of the solution (mg/L)	Size in dynamic condition (300 rpm)	UV-Vis date of magnetite in 1 st absorbance	UV-Vis date of magnetite in 2 nd absorbance
1	Fe ₃ O ₄ (MG1)	200	71.3	240.9	650.1
2	Fe ₃ O ₄ (MG2)	500	79.33	253.2	662.4
3	Fe ₃ O ₄ (MG3)	1000	82.2	257.3	670.2
4	Fe ₃ O ₄ (MG4)	2000	85.4	257.9	672.4
5	Fe ₃ O ₄ (MG5)	4000	89.9	269.3	679.5

Table 6a: 1st and 2nd UV-vis peak position with particle size in static condition [Different PVA concentration]

S.No.	Name of Sample	PVA (%)	Size in static condition	UV-Vis date of magnetite in 1 st absorbance	UV-Vis date of magnetite in 2 nd absorbance
1	Fe ₃ O ₄ (MG1)	2	82.6	254.6	670.3
2	Fe ₃ O ₄ (MG2)	4	81.8	254.8	669.2
3	Fe ₃ O ₄ (MG3)	6	80.8	254.1	668.7
4	Fe ₃ O ₄ (MG4)	8	80.7	253.4	669.0
5	Fe ₃ O ₄ (MG5)	10	77.2	252.9	660.5

Table 6b: 1st and 2nd UV-vis peak position with particle size in dynamic condition

S.No.	Name of Sample	PVA (%)	Size in dynamic condition (300 rpm)	UV-Vis date of magnetite in 1 st absorbance	UV-Vis date of magnetite in 2 nd absorbance
1	Fe ₃ O ₄ (MG1)	2	77.3	251.9	660.1
2	Fe ₃ O ₄ (MG2)	4	77.33	252.2	661.1
3	Fe ₃ O ₄ (MG3)	6	75.2	249.7	659.2
4	Fe ₃ O ₄ (MG4)	8	72.4	248.9	658.3
5	Fe ₃ O ₄ (MG5)	10	69.9	247.7	652.2

(b) UV-visible spectroscopy of hematite

In this work, synthesis of nanoparticles of hematite i.e., $\alpha\text{-Fe}_2\text{O}_3$ was done by sintering process. The magnetite was sintered at the different sintering temperature. Static and dynamic condition was utilized to prepare the nanoparticles of hematite. The size of the prepared nano particles was determined through XRD technique. UV-visible spectroscopy was used to study the absorption peak of hematite nanoparticles. Blue shift appears with decrease the sizes of the particles. The absorption peaks are slightly shifted towards the higher energy sides, when the sample was synthesized in PVA matrix.

Table 7a: 1st UV-vis peak position with particle size in static condition (in different concentration of FeCl_3)

S.No.	Name of Sample	ppm of the solution (mg/L)	Size in static condition	UV-Vis date of hematite(nm)
1	FeO. Fe_2O_3 (HT1)	200	72.6	421
2	FeO. Fe_2O_3 (HT2)	500	74.8	427
3	FeO. Fe_2O_3 (HT3)	1000	81.8	428.3
4	FeO. Fe_2O_3 (HT4)	2000	83.7	431.3
5	FeO. Fe_2O_3 (HT5)	4000	92.2	436.5

Table 7b: 1st UV-vis peak position with particle size in static condition (in different concentration of FeCl_3)

S.No.	Name of Sample	ppm of the solution (mg/L)	Size in dynamic condition (300 rpm)	UV-Vis date of hematite(nm)
1	FeO. Fe_2O_3 (HT1)	200	71.3	415
2	FeO. Fe_2O_3 (HT2)	500	79.33	428.9
3	FeO. Fe_2O_3 (HT3)	1000	82.2	428.1
4	FeO. Fe_2O_3 (HT4)	2000	75.4	422.3
5	FeO. Fe_2O_3 (HT5)	4000	83.9	427.2

Table 7a: 1st UV-vis peak position with particle size in static condition (in different concentration of PVA)

S.No.	PVA (%)	Reaction sequence	Size in static condition	UV-Vis date of hematite(nm)
1	2	$\text{Fe}_3\text{O}_4 \longrightarrow \text{FeO} \cdot \text{Fe}_2\text{O}_3$ (HT1)	82.6	432.6
2	4	$\text{Fe}_3\text{O}_4 \longrightarrow \text{FeO} \cdot \text{Fe}_2\text{O}_3$ (HT2)	81.8	428.3
3	6	$\text{Fe}_3\text{O}_4 \longrightarrow \text{FeO} \cdot \text{Fe}_2\text{O}_3$ (HT3)	80.8	426.5
4	8	$\text{Fe}_3\text{O}_4 \longrightarrow \text{FeO} \cdot \text{Fe}_2\text{O}_3$ (HT4)	80.7	426.5
5	10	$\text{Fe}_3\text{O}_4 \longrightarrow \text{FeO} \cdot \text{Fe}_2\text{O}_3$ (HT5)	77.2	427.5

Table 7b: 1st UV-vis peak position with particle size in dynamic condition (in different concentration of PVA)

S.No.	PVA (%)	Reaction sequence	Size in dynamic condition (300 rpm)	UV-Vis date of hematite(nm)
1	2	$\text{Fe}_3\text{O}_4 \longrightarrow \text{FeO} \cdot \text{Fe}_2\text{O}_3$ (HT1)	77.3	427.3
2	4	$\text{Fe}_3\text{O}_4 \longrightarrow \text{FeO} \cdot \text{Fe}_2\text{O}_3$ (HT2)	77.33	427.5
3	6	$\text{Fe}_3\text{O}_4 \longrightarrow \text{FeO} \cdot \text{Fe}_2\text{O}_3$ (HT3)	75.2	425.3
4	8	$\text{Fe}_3\text{O}_4 \longrightarrow \text{FeO} \cdot \text{Fe}_2\text{O}_3$ (HT4)	72.4	421.1
5	10	$\text{Fe}_3\text{O}_4 \longrightarrow \text{FeO} \cdot \text{Fe}_2\text{O}_3$ (HT5)	69.9	412.3

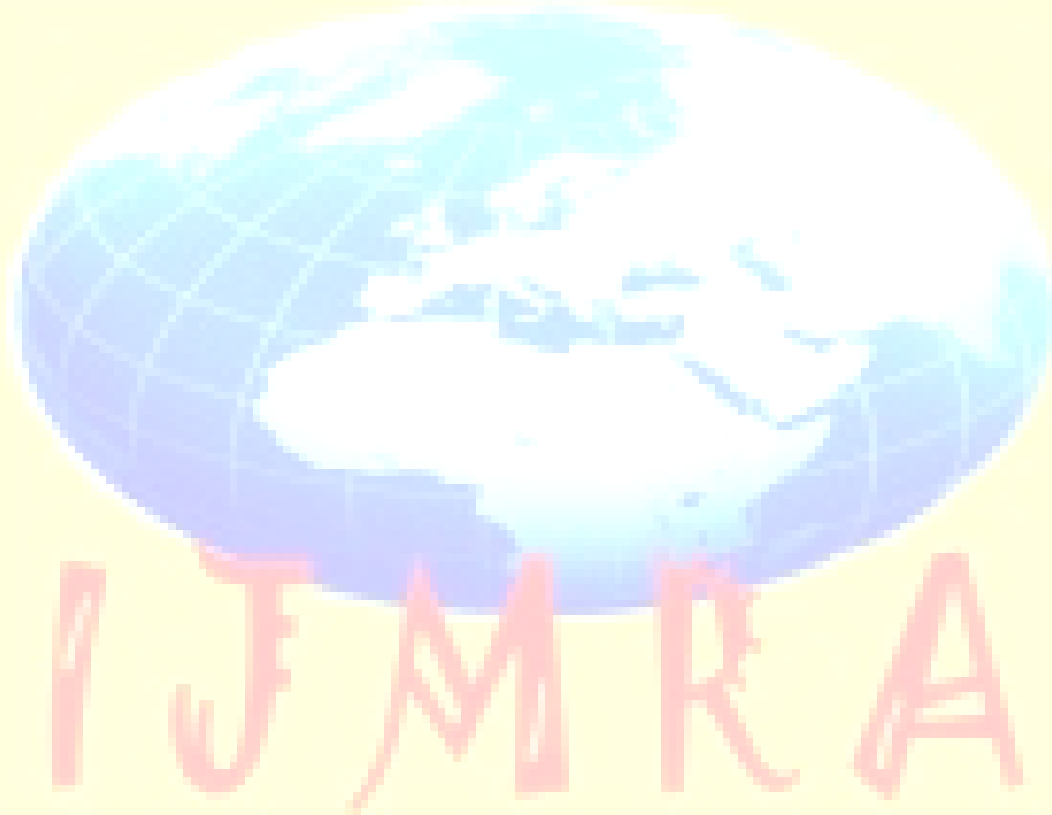
Conclusion:

Hematite and magnetite were synthesized from the chemical route technique in the presence of PVA. PVA is a water soluble polymer and form cross linked network within the water solution. Nano particle with different sizes were synthesized from the chemical route in static as well as in dynamic condition. The particle size of the magnetite varies from 72.6 to 99.2 in static condition and 71.3 to 89.9 in dynamic condition. The same result was obtained in case of hematite. FTIR was used to identify the functional group present in the materials. The main groups are Fe-O and Fe-OH. SEM again gives the reproducible result for the synthesis of the nano particles. EDAX and X-ray photoelectron spectroscopic gives the same results for the synthesis of Fe_2O_3 and Fe_3O_4 . The uv-visible spectroscopy was used to investigate the absorption characteristic of the synthesized nanoparticles. The investigation from uv-visible spectroscopy also varies from the sizes of the particles in which conditions they were synthesized. Smaller particles give the absorption at the smaller wavelength and larger particles gives at longer wavelength.

Reference:

- H. L. Zhu, Y. Duran, *J. Mater. Sci.*, 42 (2007) 9205.
- J. Toniolo, A. Takimi, *J. Mater. Sci.*, 42 (2007) 4785.
- S. Lixian, *Preparation of magnetic nanometer magnetite with the method of complex compound-hydrolyzation deposition*, School of Material Science, Southwest University of Science and Technology, (2007) Vol. 146, pp. 276982.
- H. Namduri, S. Nasazadani, *Quantitative analysis of iron oxides using fourier transform infrared spectrometry*, (2008) Vol. 50, Issue-9, pp. 2493.
- M. Ma, Y. Zhang, W. Yu, H. Shen, H. Zhang, N. Gu, Preparation and characterization of magnetite nanoparticles coated by amino silane, (2002).
- N. Mizutani, T. Iwasaki, Effect of ferrous/ferric ions molar ratio on reaction mechanism for hydrothermal synthesis of magnetite nanoparticles, (2008), pp. 713.
- Z. Yuanbi, Q. Zumin, H. Jiaying, *Chin. J. Chem. Engg.*, 451-455 (2008).

- R. Y. Honga, T. T. Pana, H. Z. Lib, *J. Magn. Magn. Mater.* 303 (2006) 60.
- Y. F. Shena, J. Tanga, Z. H. Niea, Y. D. Wanga, Y. Renc, L. Zuoa, *Preparation and application of magnetic Fe₃O₄ nanoparticles for waste water purification*, (2009) pp. 9584.
- J. Chen, F. Wang, K. Huang, Y. Liu, S. Liu, *Preparation of Fe₃O₄ nanoparticles with adjustable morphology*, (2008) pp. 898.
- B.D. Cullity, in: M. Cohen (Ed.), *Elements of X-RAY Diffraction*, 2nd ed., Addition-Wesley Publishing Company, Inc., New York, 1978, p. 102.
- Lu, J.; Jiao, X.; Chen, D.; Li, W. Solvothermal synthesis and characterization of Fe₃O₄ and γ-Fe₂O₃ nanoplates. *J. Phys. Chem. C.* 2009, 113, 4012-4017.



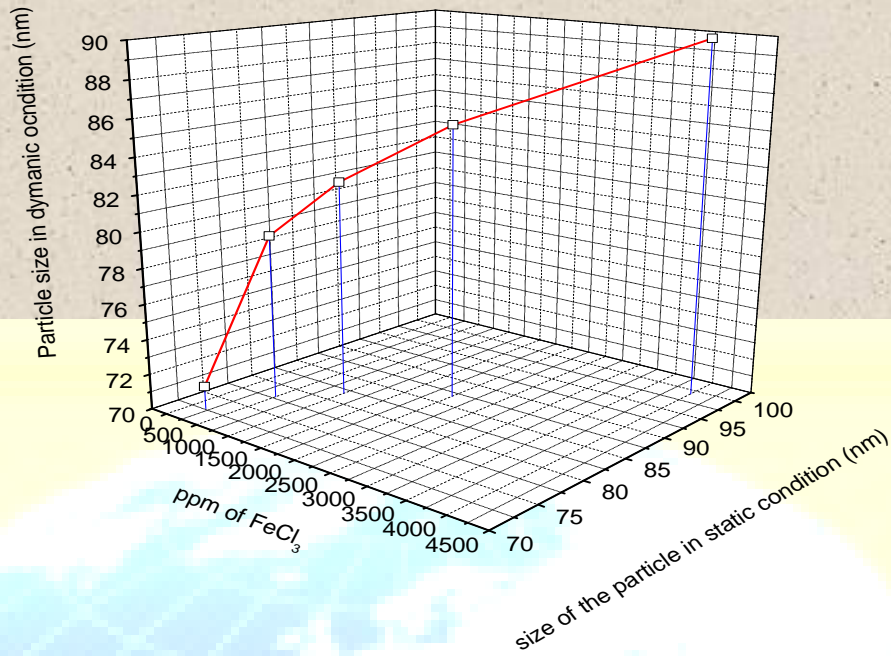


Fig1. Variation of the particle size with the volume percentage of FeCl₃

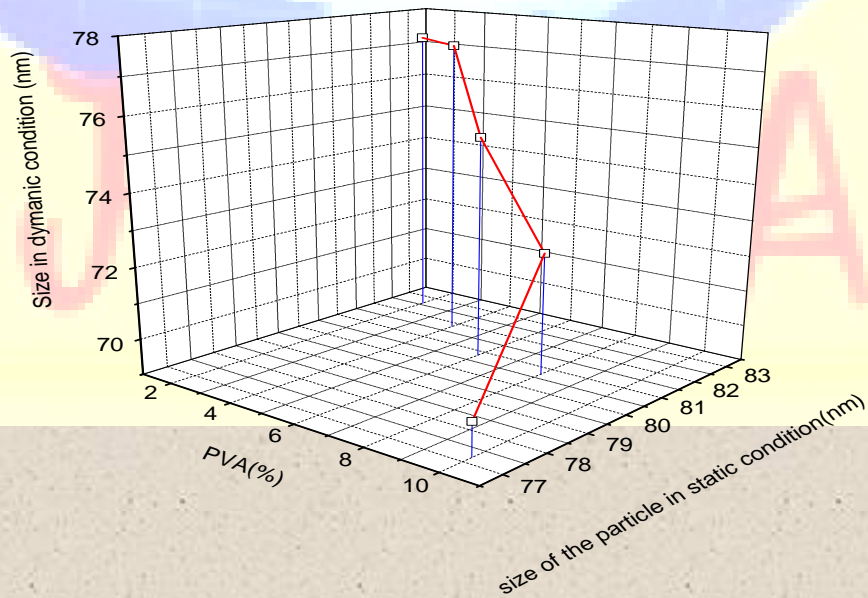


Fig 2. Variation of the particle size with the volume percentage of PVA

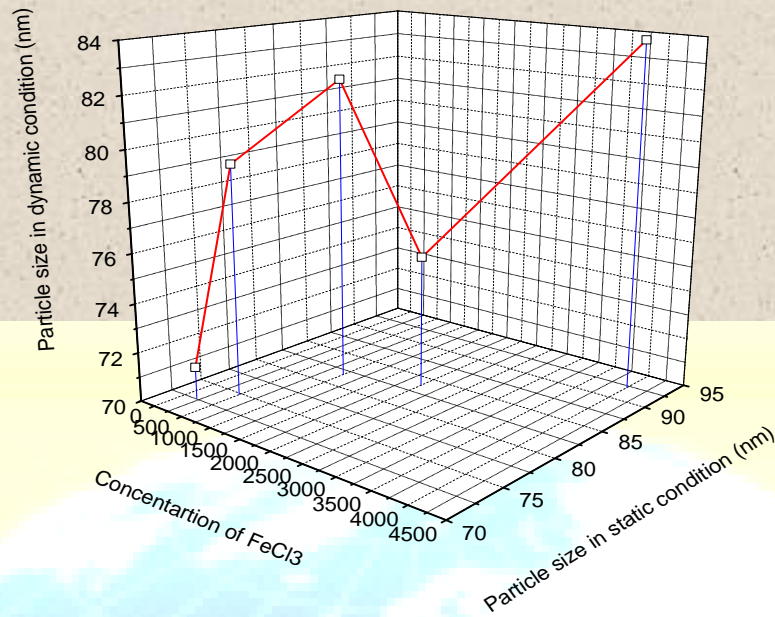


Fig3. Variation of the particle size with the volume percentage of FeCl₃ (HM)

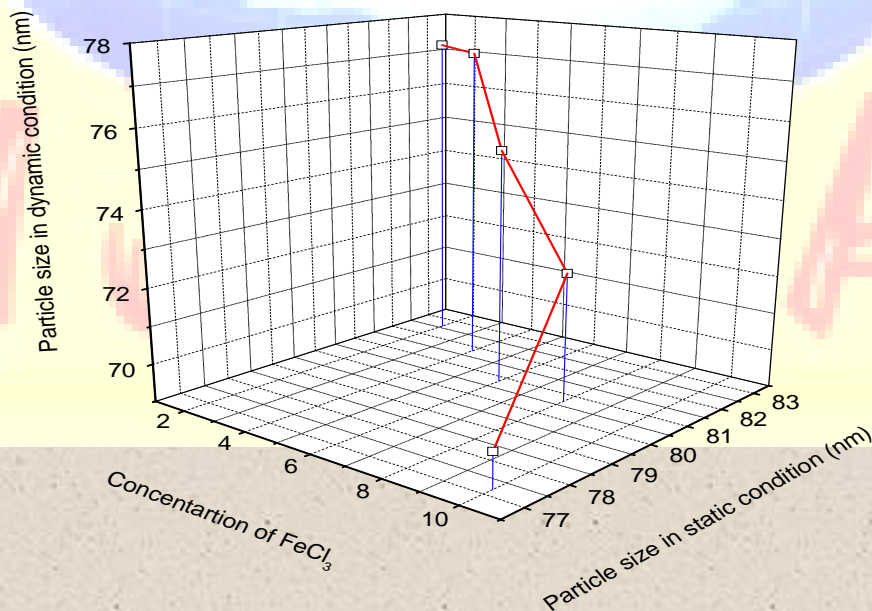


Fig 4 Variation of the particle size with the volume percentage of PVA

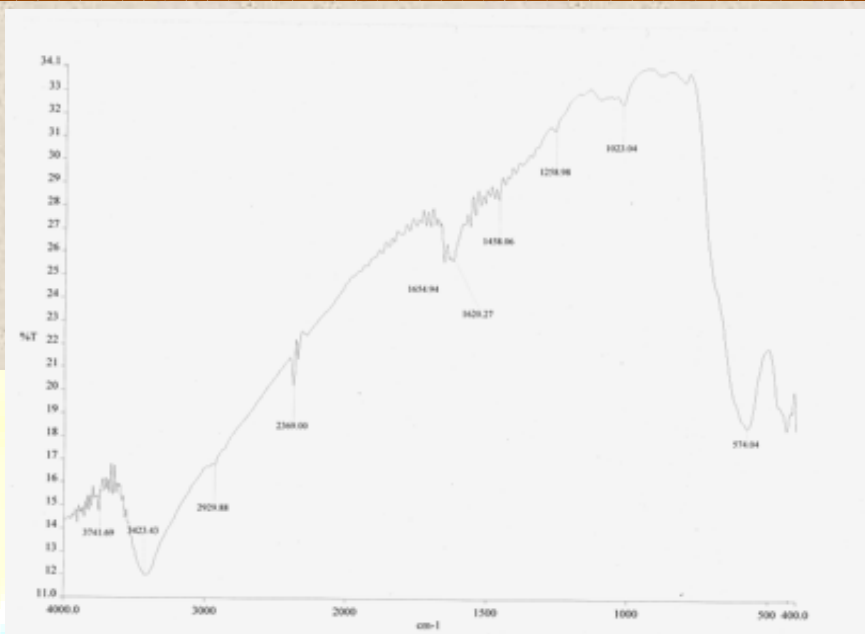


Fig. 5 FT-IR spectrum of magnetite NPs

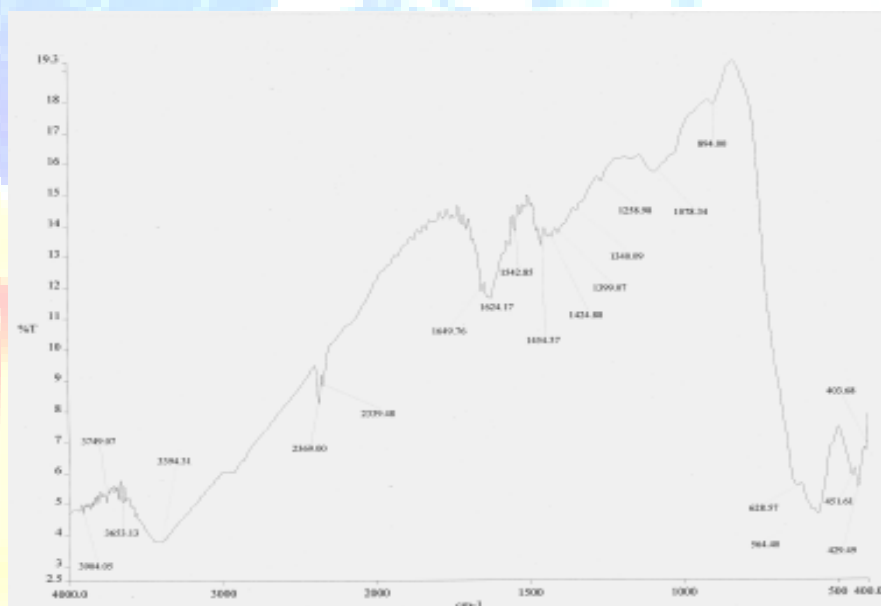


Fig. 6 FT-IR spectrum of hematite NPs

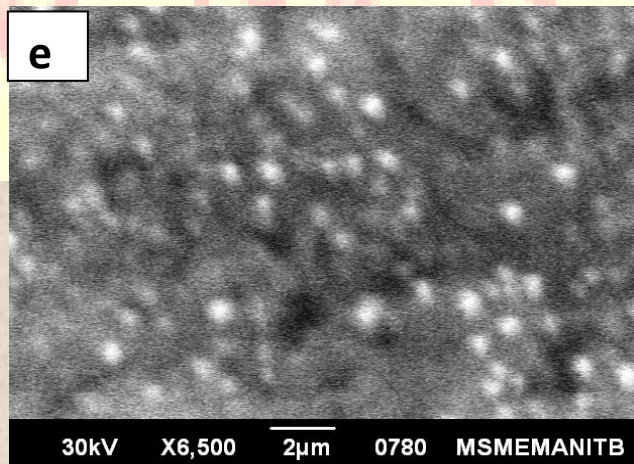
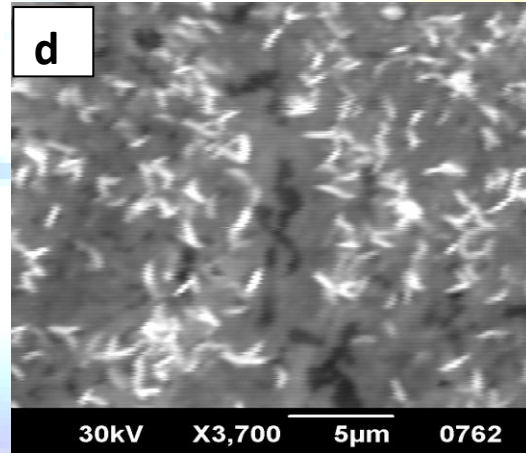
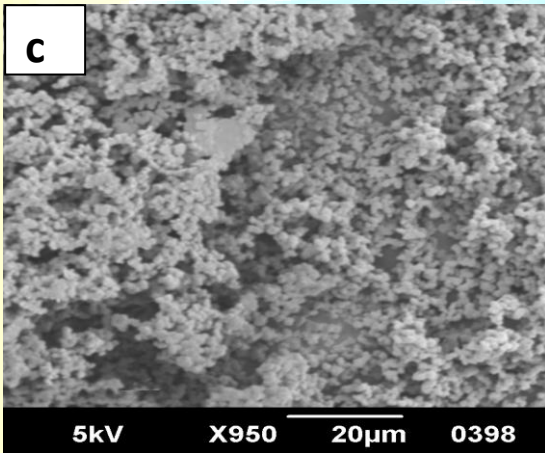
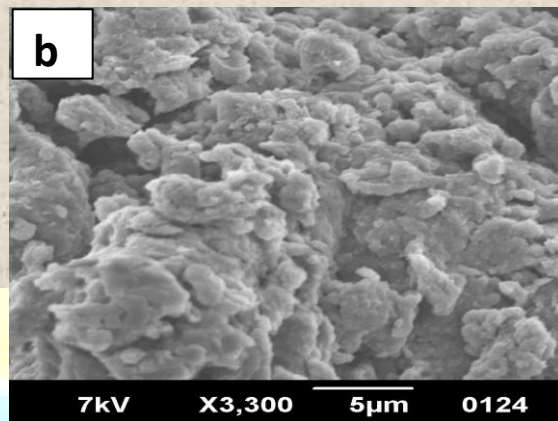
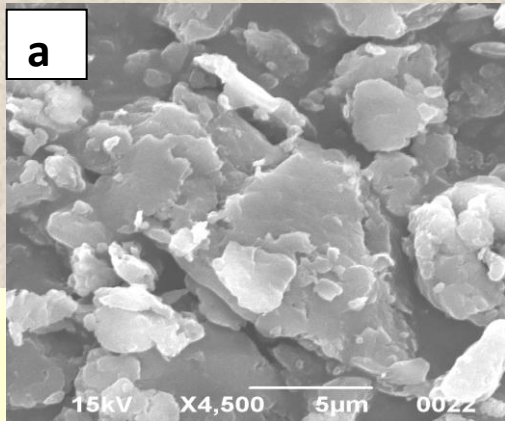


Fig. 8 SEM image of hematite NPs at the different magnification

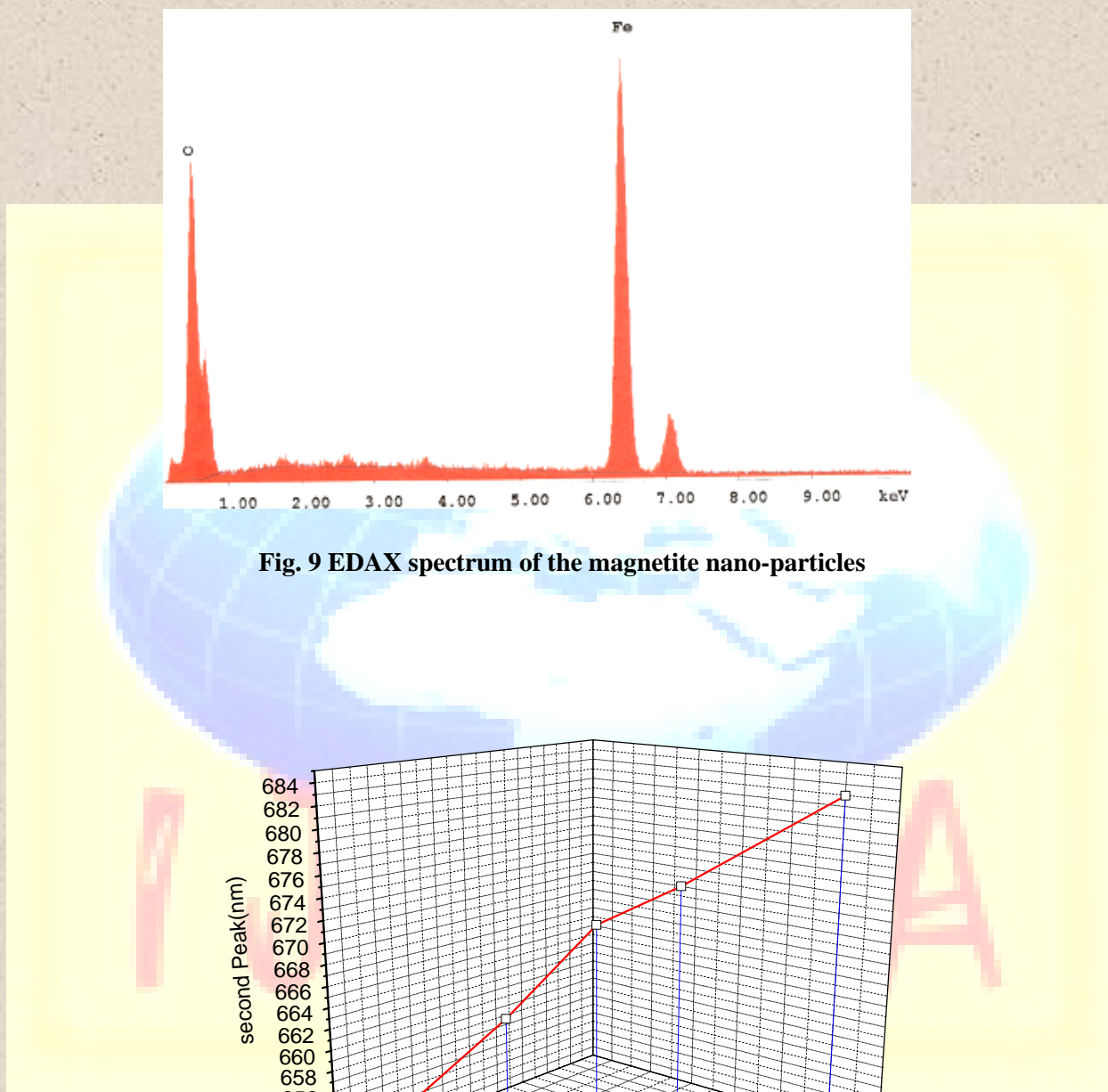
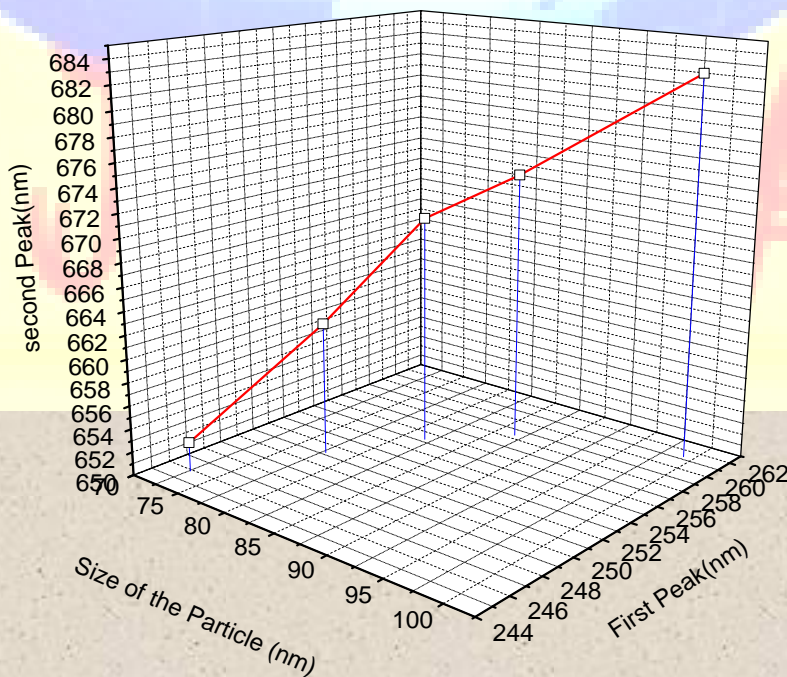
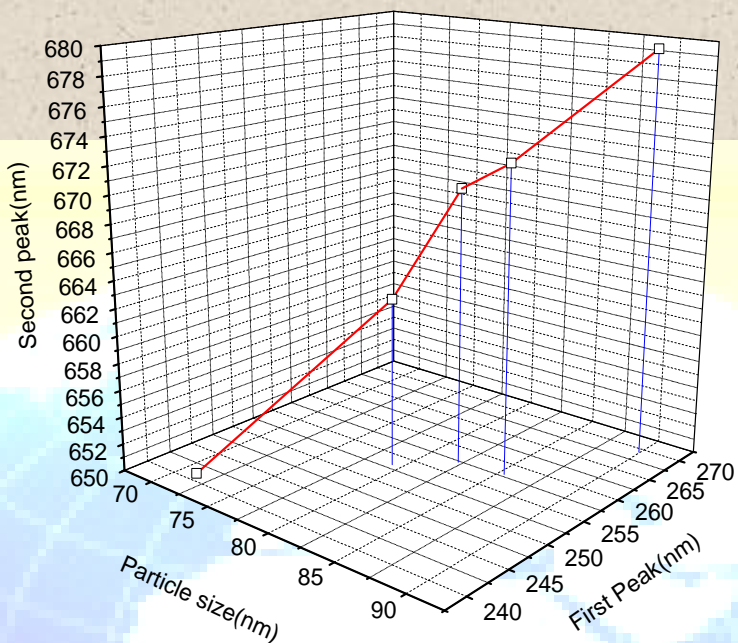


Fig. 9 EDAX spectrum of the magnetite nano-particles

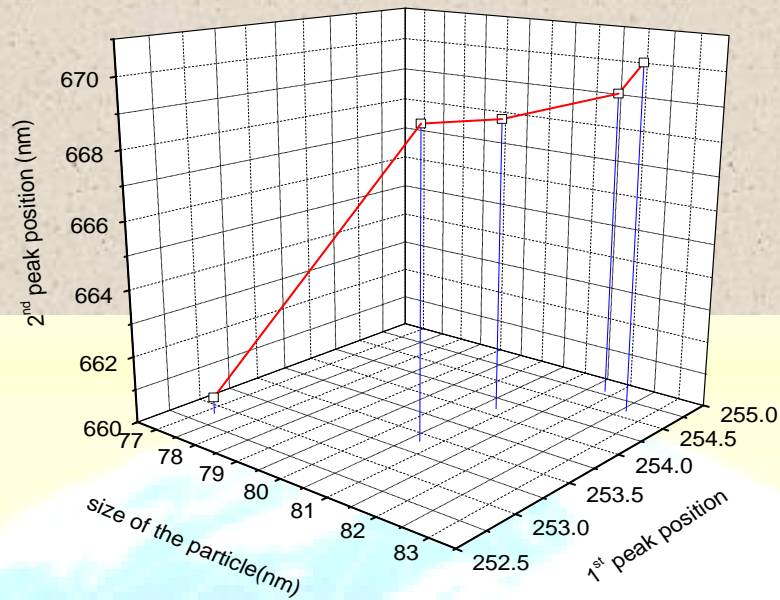


(a)

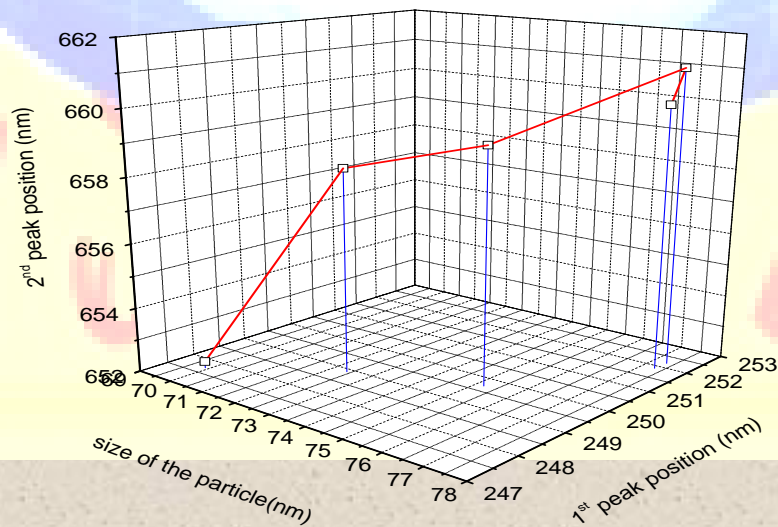


(b)

Fig 10 Variation of 1st and 2nd UV-vis peak band of magnetite with the size (a) static condition (b) dynamic condition [Different FeCl₃ concentration]



(a)



(b)

Fig 11 Variation of 1st and 2nd UV-vis peak band of hematite with the size (a) static condition (b) dynamic condition [Different PVA concentration]

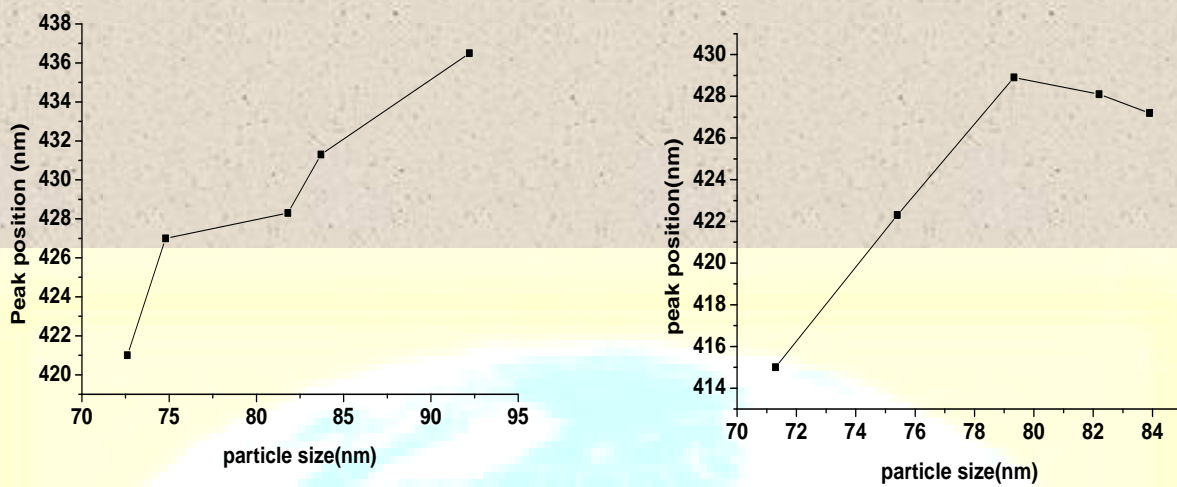


Fig 12 Variation of 1st and 2nd UV-vis peak band with the size (a) static condition (b) dynamic condition [Different FeCl₃ concentration].

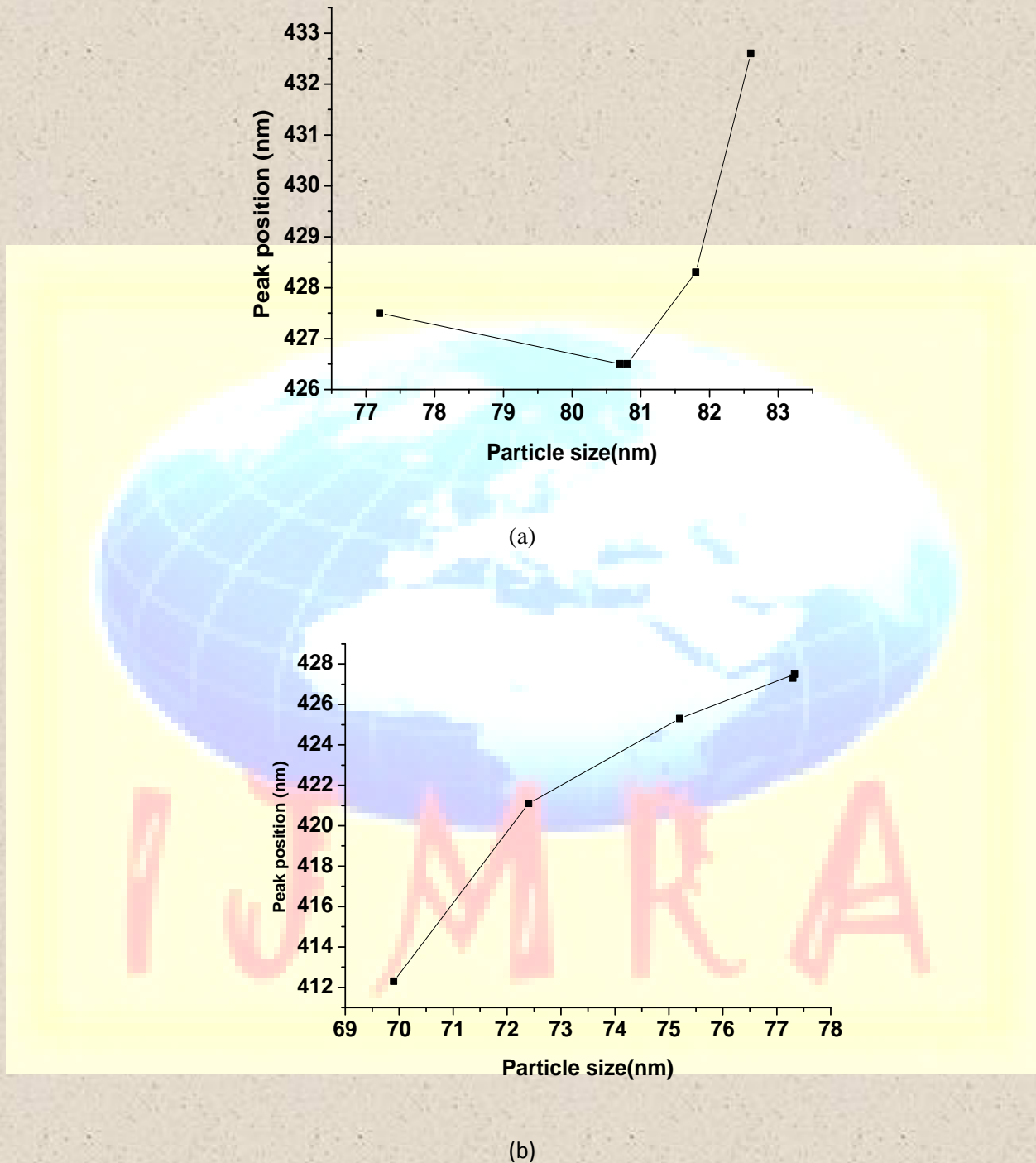


Fig 13 Variation of 1st and 2nd UV-vis peak band with the size (a) static condition (b) dynamic condition [Different PVA concentration]